AIP Journal of Applied Physics

InAs quantum dot growth on Al x Ga1 − x As by metalorganic vapor phase epitaxy for intermediate band solar cells

R. Jakomin, R. M. S. Kawabata, R. T. Mourão, D. N. Micha, M. P. Pires, H. Xie, A. M. Fischer, F. A. Ponce, and P. L. Souza

Citation: Journal of Applied Physics **116**, 093511 (2014); doi: 10.1063/1.4894295
View online: http://dx.doi.org/10.1063/1.4894295
View Table of Contents: http://scitation.aip.org/content/aip/journal/jap/116/9?ver=pdfcov
Published by the AIP Publishing

Articles you may be interested in

InGaAs/GaAsP superlattice solar cells with reduced carbon impurity grown by low-temperature metal-organic vapor phase epitaxy using triethylgallium
J. Appl. Phys. **116**, 203101 (2014); 10.1063/1.4902319

Effect of spacer layer thickness on multi-stacked InGaAs quantum dots grown on GaAs (311)B substrate for application to intermediate band solar cells
J. Appl. Phys. **111**, 074305 (2012); 10.1063/1.3699215

Narrow band gap (1 eV) InGaAsSbN solar cells grown by metalorganic vapor phase epitaxy
Appl. Phys. Lett. **100**, 121120 (2012); 10.1063/1.3693160

Metal organic vapor-phase epitaxy of InAs/InGaAsP quantum dots for laser applications at 1.5 μm
Appl. Phys. Lett. **99**, 101106 (2011); 10.1063/1.3634029

Bimodal distribution of Indium composition in arrays of low-pressure metalorganic-vapor-phase-epitaxy grown InGaAs/GaAs quantum dots
Appl. Phys. Lett. **79**, 2157 (2001); 10.1063/1.1406553

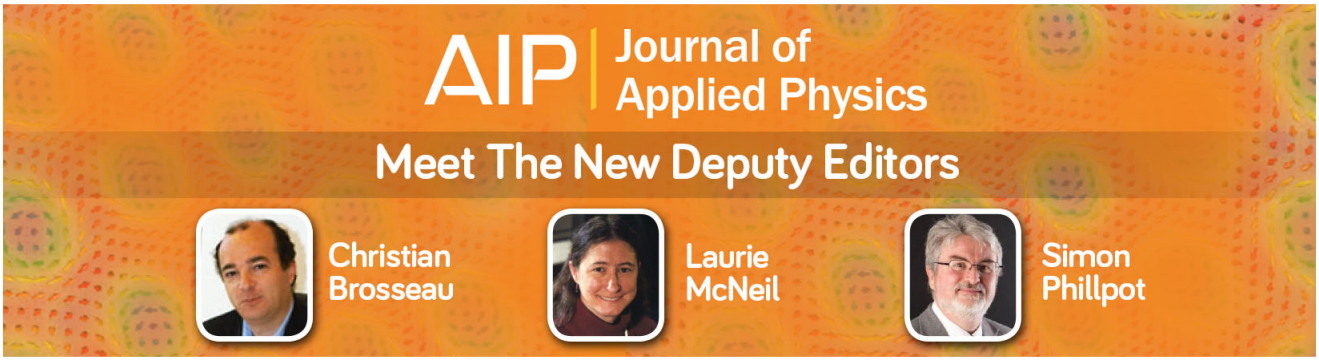

[This article is copyrighted as indicated in the article. Reuse of AIP content is subject to the terms at: http://scitation.aip.org/termsconditions. Downloaded to] IP: 149.169.162.2 On: Tue, 17 Feb 2015 22:23:12

JOURNAL OF APPLIED PHYSICS **116**, 093511 (2014)

InAs quantum dot growth on $Al_xGa_{1-x}As$ by metalorganic vapor phase epitaxy for intermediate band solar cells

R. Jakomin,[1,2,a)] R. M. S. Kawabata,[2,3] R. T. Mourão,[2,4] D. N. Micha,[2,4,5] M. P. Pires,[2,4] H. Xie,[6] A. M. Fischer,[6] F. A. Ponce,[6] and P. L. Souza[2,3]
[1]*Campus de Xerém, Universidade Federal do Rio de Janeiro, UFRJ, Duque de Caxias-RJ, Brazil*
[2]*Instituto Nacional de Ciência e Tecnologia de Nanodispositivos Semicondutoires–DISSE–PUC-Rio, RJ, Brazil*
[3]*Pontificia Universidade Católica do Rio de Janeiro, Marques de São Vicente 225, Rio de Janeiro, 22452-900 RJ, Brazil*
[4]*Instituto de Física, Universidade Federal do Rio de Janeiro, UFRJ, Rio de Janeiro-RJ, Brazil*
[5]*Coordenação de Licenciatura em Física, CEFET/RJ, Petrópolis-RJ, Brazil*
[6]*Department of Physics, Arizona State University, Tempe, Arizona 85287-1504, USA*

(Received 1 July 2014; accepted 19 August 2014; published online 4 September 2014)

InAs quantum dot multilayers have been grown using $Al_xGa_{1-x}As$ spacers with dimensions and compositions near the theoretical values for optimized efficiencies in intermediate band photovoltaic cells. Using an aluminium composition of $x = 0.3$ and InAs dot vertical dimensions of 5 nm, transitions to an intermediate band with energy close to the ideal theoretical value have been obtained. Optimum size uniformity and density have been achieved by capping the quantum dots with GaAs following the indium-flush method. This approach has also resulted in minimization of crystalline defects in the epilayer structure. © *2014 AIP Publishing LLC*.
[http://dx.doi.org/10.1063/1.4894295]

I. INTRODUCTION

Self-assembled InAs quantum dots (QDs) grown on $Al_xGa_{1-x}As$ layers have attracted much attention in the last two decades, especially for applications in optoelectronic devices such as lasers and photodetectors.[1–3] The formation of self-assembled QDs using molecular beam epitaxy (MBE) and metalorganic vapor phase epitaxy (MOVPE) techniques is facilitated by the strain-induced Stranski-Krastanov growth mode. Difficulties in the growth of InAs QDs on (Al)GaAs by MOVPE include the tendency for clusters formation and post-growth morphology evolution.[4,5] Ripening of QDs for diode laser applications has been observed using *in-situ* scanning tunneling microscopy.[6] A higher surface diffusion in MOVPE, compared to MBE, induces a faster QD formation that can lead to island coalescence, and a bimodal QD size distribution.[7,8]

Stacked layers have been employed in optoelectronic applications in order to enhance the three-dimensional confinement effects. However, strain accumulation must be considered and preferably minimized to prevent plastic deformation and consequent surface roughness, which can affect the formation of QDs and deteriorate the optical properties. Strained and defective regions induce different growth rates[9] modifying the QD size and producing a multimodal height distribution. One method to reduce the QD size distribution in stacked self-assembled QDs is by flushing out traces of indium at a desired GaAs capping thickness, in what is also known as the *indium-flush* method.[10] This approach has demonstrated sharp photoluminescence (PL) peaks and an increase in electron confinement due to higher uniformity in QD height.

Intermediate band solar cells (IBSC) have received special attention as an approach to improve the energy conversion efficiency of conventional tandem solar cells.[11] One way to create an intermediate band is via the overlap of the confined states in quantum dots. The formation of an intermediate energy band allows the generation of additional electrons and holes by absorption of two sub-bandgap energy photons, which would not normally be absorbed in a standard single-junction solar cell. In addition to the ordinary transition from the valence band to the conduction band across the bandgap (E_G), the QDs provide possible transitions from the valence band to an intermediate band (E_M) and from the intermediate band to the conduction band (E_L). The development of QD-IBSCs has been based mainly on the InAs/GaAs system due to the mature knowledge of growth conditions, despite the fact that the bandgap of GaAs ($E_G = 1.42$) differs from the ideal value derived from the detailed balance model ($E_G = 1.95$ eV, and sub-bandgaps of $E_L = 0.71$ eV and $E_M = 1.24$ eV).[12]

A better match to the solar spectrum can be achieved by replacing GaAs with $Al_xGa_{1-x}As$ spacers.[13] With a maximum lattice mismatch of only 0.1%, $Al_xGa_{1-x}As$ can be easily grown on a GaAs substrate, and a similar strain-induced Stranski-Krastanov growth mode can be expected for InAs QDs on this alloy. There are only a few studies of InAs QDs grown on $Al_{1-x}Ga_xAs$, particularly by MOVPE, and a careful investigation is needed. In order to produce efficient QD-IBSCs, a high density and a uniform size-distribution of QDs are required. In fact, size dispersion limits the absorption efficiency for the different transitions and can cause an undesired absorption coefficient overlap between the

[a)]Author to whom correspondence should be addressed. Electronic mail: robertojakomin@xerem.ufrj.br. Tel.: +55(21)35272197.

 © 2014 AIP Publishing LLC

[This article is copyrighted as indicated in the article. Reuse of AIP content is subject to the terms at: http://scitation.aip.org/termsconditions. Downloaded to] IP: 149.169.162.2 On: Tue, 17 Feb 2015 22:23:12

sub-bandgap transitions.[14] Furthermore, particular attention must be paid on strain fields introduced by the QDs in order to avoid plastic deformation effects.

In this work, we report on a study of the growth by MOVPE of InAs QDs on $Al_xGa_{1-x}As$ layers for QD-IBSC applications. The $Al_xGa_{1-x}As$ barrier composition has been selected to optimize cell efficiency based on a detailed balance model.[12] We show that bimodal size-distribution is very much attenuated at low growth temperatures and high growth rates. In order to achieve a more appropriate fabrication procedure for the stacked structure, we have examined two QD covering methods using GaAs and have observed that threading dislocations can be minimized when the original deposited dots are first only partially covered. The influence of the growth conditions on QD morphology and on the structural and optical characteristics has been analyzed by atomic force microscopy (AFM), transmission electron microscopy (TEM), reflectance anisotropy spectroscopy (RAS), and PL.

II. EXPERIMENTAL DETAILS

The MOVPE growth was performed in an Aixtron AIX-200 (1″ × 2″) horizontal reactor at 100 mbar on *n*-doped (001) GaAs substrates. The hydrogen carrier gas flow was optimized for maximum growth homogeneity, at a total flow rate of 8 l/min. The tri-methyl aluminum (TMAl) and tri-methyl gallium (TMGa) precursors were calibrated for growth of $Al_{0.3}Ga_{0.7}As$ with a growth rate of ~0.9 nm/s, a V/III ratio of 17, and a growth temperature of 630 °C. To reach 30% of Al content, the TMAl flow was adjusted to an Al/III gas phase ratio of 0.27. Room-temperature photoluminescence gave a bandgap of 1.83 eV for these layers. To maximize the QD density, we optimized growth parameters such as growth rate, thickness, post-growth annealing time, and V/III ratios. We have studied temperatures for QD growth ranging between 480 and 520 °C. Two QD covering methods were used to investigate the generation of dislocations and the QD height uniformity. The first method (Method A) consists of depositing a low-temperature 5-nm-thick GaAs layer in order to truncate and partially cover the InAs QDs (i.e., using the *In-flush* method), flushing out the In atoms on the top of the dots that exceed the approximate 5 nm height.[10] The second method (Method B) consists of completely covering the InAs QDs with a low-temperature 20-nm-thick GaAs layer. The full active region of the QD-IBSC structure consists of 10 layers of InAs QDs (covered either by methods A or B) separated by a 90-nm-thick $Al_{0.3}Ga_{0.7}As$ barrier.

RAS measurements were performed during growth, using a Laytec EpiRAS 2000 tool. In order to study the QD surface reconstruction immediately after growth, measurements were performed in spectroscopic mode at 400 °C, which is lower than the QD growth temperature, to prevent surface reconstruction evolution during the measurements. The chosen energy range for the RAS measurement was between 1.50 and 4.00 eV with a 0.01 eV step. The QD layers were analyzed using a Veeco MultiMode V AFM in tapping mode. The AFM tip was driven at frequencies higher than 100 KHz. The surfaces were then mapped on 2 μm × 2 μm topography images, with a height accuracy of 0.5 nm.

The microstructure was studied by TEM with an electron accelerating voltage of 400 kV. The cross-section TEM samples were prepared for observation along a ⟨110⟩ crystal projection, using standard mechanical polishing techniques followed by ion milling at shallow angles with a 5 kV Ar^+ ion beam. Diffraction contrast and multi-beam axial images were obtained to determine the atomic arrangement in the QDs and the nature of associated extended defects and interfaces. The optical properties were studied by PL spectroscopy, at a temperature of 10 K, using a 532-nm 10-mW laser and a liquid-nitrogen-cooled Ge detector.

III. RESULTS AND DISCUSSION

A. Theoretical model

The IBSC concept for the InAs QD/GaAs system has been investigated over the past few years. The absorption of sub-bandgap photons and the possibility of minimal degradation of the open circuit voltage in comparison with single junction GaAs solar cells have been reported.[15–17] The absorption energies for the InAs/GaAs system are, in principle, $E_G = 1.4$ eV, $E_M = 1$ eV, and $E_L = 0.4$ eV. However, the experimentally observed energies are 1.2, 1.0, and 0.2 eV, respectively, reportedly due to thermal escape and wetting layer effects.[18] As previously mentioned, the detailed balance model for QD-IBSCs shows a maximum conversion efficiency of 63% for an ideal photovoltaic device with $E_G = 1.95$ eV, $E_M = 1.24$ eV, and $E_L = 0.71$ eV.[12] We have replaced GaAs with $Al_xGa_{1-x}As$ in order to achieve a host-material bandgap closer to the theoretical ideal, as well as a higher conduction band offset, without deteriorating the QD quality. The bandgap of InAs on GaAs has been calculated as 0.418 and 0.785 eV for relaxed and pseudomorphically strained epitaxial conditions.[19] Since the AlGaAs lattice parameter is essentially the same as for GaAs, we use the same InAs temperature-dependent energy gap values in the equation

$$E_{gap}^{strained\ InAs}(T) = \{0.785\text{–}2.76 \times 10^{-4}\,T^2/(T+93)\}\text{eV}. \tag{1}$$

On the other hand, the $Al_xGa_{1-x}As$ bandgap as a function of Al concentration and temperature is given as

$$\begin{aligned} E_{gap}^{AlxGa1-xAs}(x,\,T) &= \{x[3.13 - 8.85 \times 10^{-4}\,T^2/(T+530)] \\ &\quad + (1-x)[1.519 - 5.4 \times 10^{-4}\,T^2/(T+204)] - x \\ &\quad \times (1-x)(1.31x - 0.127)\}\,\text{eV}, \end{aligned} \tag{2}$$

where we use published energy gap values for strained InAs[19] and for GaAs and AlAs.[21] The Varshni and the bowing correction parameters were taken from Ref. 20. Considering a conduction band offset of 70% of the difference in band gap, the electronic quantum levels of the InAs QD/$Al_xGa_{1-x}As$ system were estimated and the relative transition energies extracted from the energy differences between VB and IB (E_M), IB and CB (E_L), and VB and CB (E_G) as depicted in Fig. 1(a).[19] It is worth noting that the E_M and E_L energy transitions are only approximate reference

[This article is copyrighted as indicated in the article. Reuse of AIP content is subject to the terms at: http://scitation.aip.org/termsconditions. Downloaded to] IP: 149.169.162.2 On: Tue, 17 Feb 2015 22:23:12

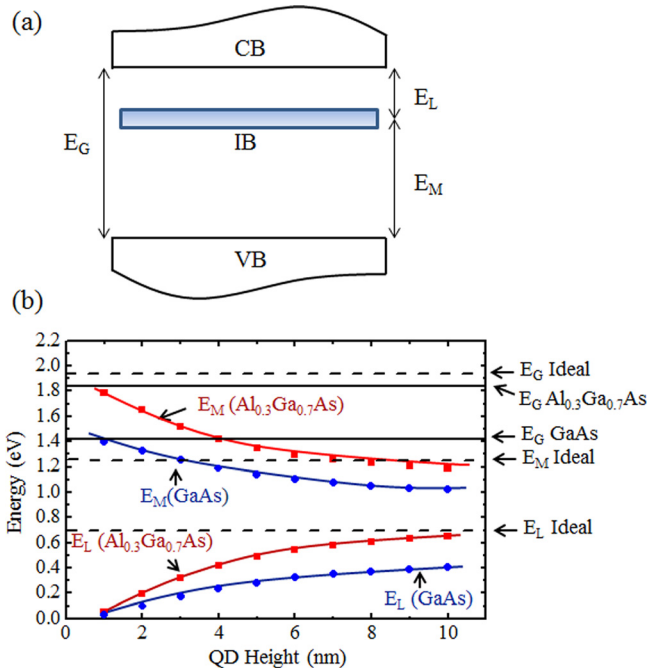

FIG. 1. Theoretical model of an intermediate-band solar cell structure. (a) Band energy diagram showing the three different energy transitions for the IBSC. (b) Transition energies at room temperature as a function of the QD height for InAs QD/$Al_{0.3}Ga_{0.7}As$ (squares) and GaAs (circles). The horizontal dashed lines indicate the ideal energy values for the IBSC applications. The horizontal solid lines indicate the $Al_{0.3}Ga_{0.7}As$ and GaAs energy gaps.

values. In the presence of an intermediate band, the transitions should be more properly represented by energy ranges. For the simulations, we used a Schrodinger equation solver based on the split-operator model in the one-dimensional effective mass approximation model.[22] The calculated values of E_G, E_M, and E_L as a function of QD height are shown in Fig. 1(b) for $Al_{0.3}Ga_{0.7}As$ and GaAs barriers at 300 K. For a solar cell operating at 300 K, a perfect match for all three ideal energies is not possible at any Al concentration. E_M is near the ideal value of 1.24 eV for a QD height around 6 nm, while E_L (at 0.55 eV) is less than the 0.71 eV ideal. On the other hand, by increasing the QD height to 10 nm, E_L approaches the ideal while E_M (at 1.1 eV) is less than the optimum value. For QD heights larger than 5 nm, a second bound state appears inside the confining potential, thus QD heights of about 5 nm should be chosen in order to optimize the IB-CB transition. The Al concentration in the barrier material has a pronounced influence on the E_G and E_L transitions. The difference between the E_M transitions for GaAs and $Al_{0.3}Ga_{0.7}As$ becomes smaller with increasing QD height. In Fig. 1(b), the E_G values for the $Al_{0.3}Ga_{0.7}As$ and GaAs barriers are depicted as horizontal solid lines. The horizontal dashed lines represent the ideal transition energies for QD-IBSCs. Luque and Martí calculated that the conversion efficiency is above 60% even if there is a difference of ±200 meV for the E_L value and ±400 meV for the E_G value.[11] We observe in Table I that the use of $Al_{0.3}Ga_{0.7}As$ almost satisfies these conditions at 300 K while GaAs does not (a difference of around 220 meV and 110 meV vs. 430 meV and 530 meV, respectively, for a height of 5 nm). $Al_{0.3}Ga_{0.7}As$ does not present the ideal energy gap at room temperature (1.84 eV vs 1.95 eV). The ideal energy gap would be reached by an $Al_{0.4}Ga_{0.6}As$ barrier material, but in this case an E_M of around 1.4 eV, larger than the ideal 1.24 eV, would be expected. The choice of $Al_{0.3}Ga_{0.7}As$ is based on a compromise between E_G and E_M optimization.

TABLE I. Energy values for the intermediate-band model, corresponding to an InAs QD with 5 nm height and surrounded with GaAs and $Al_{0.3}Ga_{0.7}As$. The values corresponding to room and low temperatures were obtained using Eq. (2) and simulations with a Schrodinger equation solver based on the split-operator model in the one-dimensional effective mass approximation model.[21]

	T = 300 K		T = 0 K		
	$Al_{0.3}Ga_{0.7}As$	GaAs	$Al_{0.3}Ga_{0.7}As$	GaAs	Ideal
E_L	0.49	0.28	0.51	0.3	0.71
E_M	1.35	1.14	1.43	1.22	1.24
E_G	1.84	1.42	1.94	1.52	1.95

B. Growth of InAs QDs on $Al_xGa_{1-x}As$

We first deposit one layer of InAs QDs on $Al_{0.3}Ga_{0.7}As$, while varying several growth parameters in order to maximize the QD density and to improve the size uniformity. In all our growth attempts, we have observed a bimodal QD size distribution in the AFM images, consisting of small and large dots, the latter showing strain relaxation that may result in threading dislocations. The formation of a bimodal size distribution has been reported for InAs/GaAs and for other material systems.[7,23] It is attributed to the higher growth rate of the relaxed islands as compared to that of the strained pseudomorphic islands.[8]

To establish a criterion to compare size uniformity of different samples, a homogeneity parameter is defined as the ratio between the density of one group of QDs and the total QD density. The total QD density typically decreases as the growth temperature increases, as shown in Fig. 2. This behavior is expected to be due to the surface adatom diffusion length increasing with temperature, favoring coalescence of existing clusters, and resulting in a lower density of larger QDs.

The influence of growth rate (i.e., TMIn flow) on the QD density is shown in Fig. 3. A maximum density is reached for a TMIn flow of 175 sccm (1 ML/s), which corresponds to a relatively low V/III ratio of 6.4. Further reduction of the V/III ratio increases the In adatom mobility on the surface due to the low density of As atoms,[24,25] decreasing the QDs density and increasing their size. Best conditions for QD-IBSCs were found to be for QD growth at 490 °C and at a rate of 1 ML/s, resulting in a QD density of $1.7 \times 10^{10}/cm^2$ and a homogeneity of 49%. Under these conditions, the formation of clusters and large QDs is inhibited.

C. QDs capping layer study

Three structures were studied in order to understand the effect of the QD capping layer on the structural and optical characteristics. One reference structure consists of a layer with InAs QDs deposited on $Al_{0.3}Ga_{0.7}As$ with no capping layer. The other two structures consist of stacks of five InAs

[This article is copyrighted as indicated in the article. Reuse of AIP content is subject to the terms at: http://scitation.aip.org/termsconditions. Downloaded to] IP: 149.169.162.2 On: Tue, 17 Feb 2015 22:23:12

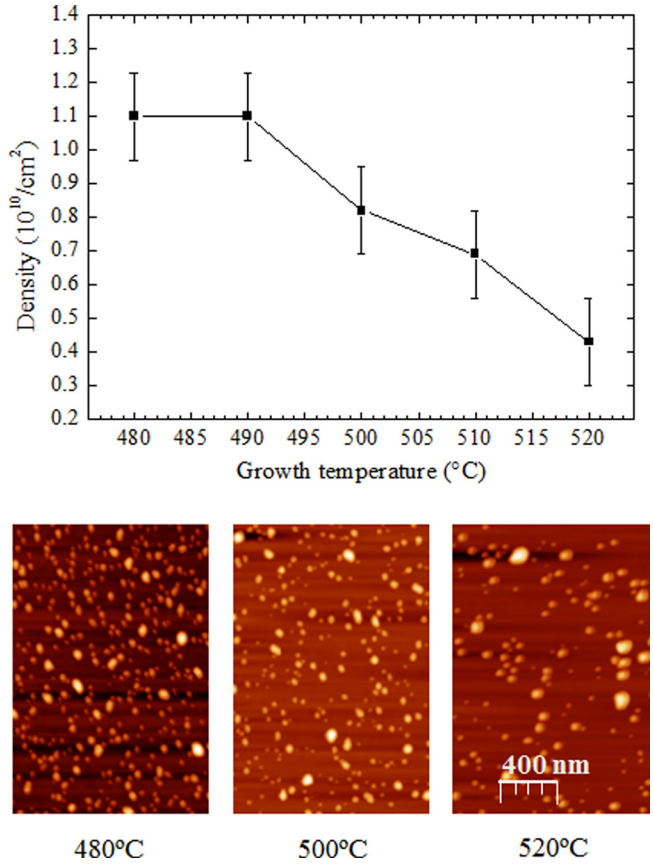

FIG. 2. Morphology of QDs measured by atomic force microscopy. (a) QD density as a function of the growth temperature. The solid line is just a visual guide. (b) Surface morphology for different growth temperatures, obtained by AFM for InAs/$Al_{0.3}Ga_{0.7}As$ QDs.

QD layers, one grown with method A and the other with method B. The QD layers are separated by ~90-nm thick $Al_{0.3}Ga_{0.7}As$ layers. The top InAs QD layer was left uncovered in order to perform AFM measurements. Fig. 4 shows the height distribution histograms of these three samples. As observed, the capping method has a clear influence on the QDs height distribution of the top layer. The QDs density and size uniformity are preserved for the structure grown with method A as shown in Figs. 4(a) and 4(b). The Gaussian fit of the histogram gives an average height of about 5 nm, taking into consideration a wetting layer about

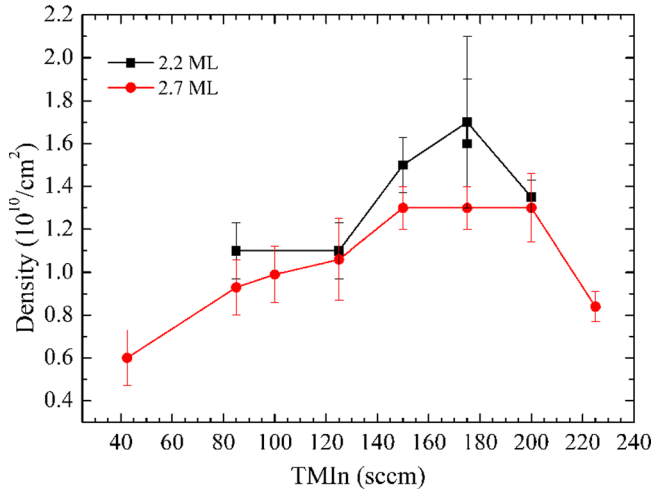

FIG. 3. Effect of flow rate and V/III ratio on the density of QDs. QD density of InAs/$Al_{0.3}Ga_{0.7}As$ as a function of TMIn flow (corresponding to a growth rate range between 0.2 and 1.2 ML/s) for different thickness (2.2 and 2.7 ML) and at a growth temperature of 490 °C, annealing time of 12 s and AsH_3 flow of 5 sccm.

1 nm thick. In contrast, the structure grown with method B shows no uniformity in the QDs density and size as depicted in Fig. 4(c), with the presence of a significant number of larger islands (with more than 10 nm in height). These results demonstrate that the use of an In-flush method favors QD size uniformity, even when QD layers are spatially separated by $Al_{0.3}Ga_{0.7}As$ layers.

TEM images of 10 layer structures grown following coverage method A (using In-flush after deposition of a 5 nm cap layer) and method B (not using In-flush and the temperature being raised only when all dots are covered) are shown in Fig. 5. These images were taken along a ⟨110⟩ projection. The QDs are generally lens-shaped and not vertically aligned. The lateral length of the QDs ranges from 10 nm to 50 nm. For fully relaxed InAs on GaAs, with a lattice mismatch of 6.8%, Lomer dislocations should be present with a separation of 6.04 nm, representing the termination of {110} planes from the GaAs side. The Fourier filtered image of the smaller dot with a diameter ~15 nm in Fig. 6(a) shows no missing {110} planes on the InAs side, i.e., it presents a pseudomorphic (coherently strained) InAs/GaAs interface. The larger dots do exhibit misfit strain relaxation via 60°

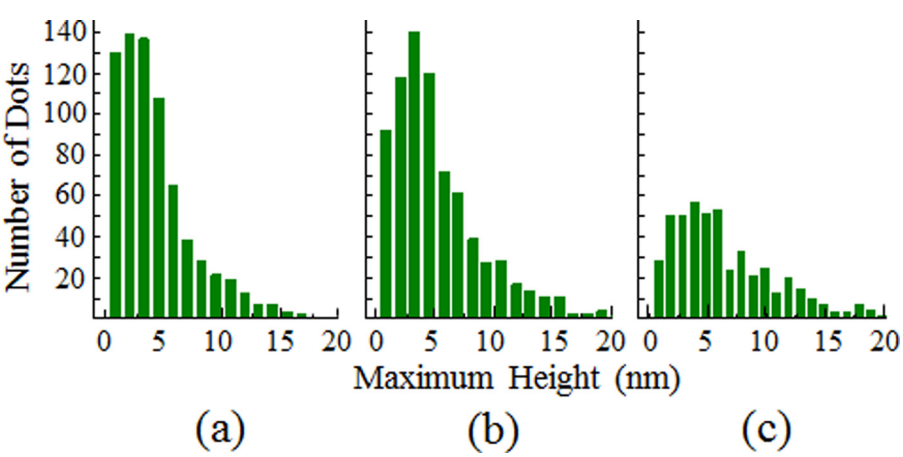

FIG. 4. Height distribution histogram for the top layer of InAs/$Al_{0.3}Ga_{0.7}As$ QDs: (a) no capping layer (only 1 QD top layer); (b) after capping method A of a stacked 5-layer structure; and (c) after capping method B of a stacked 5-layer structure.

[This article is copyrighted as indicated in the article. Reuse of AIP content is subject to the terms at: http://scitation.aip.org/termsconditions. Downloaded to] IP: 149.169.162.2 On: Tue, 17 Feb 2015 22:23:12

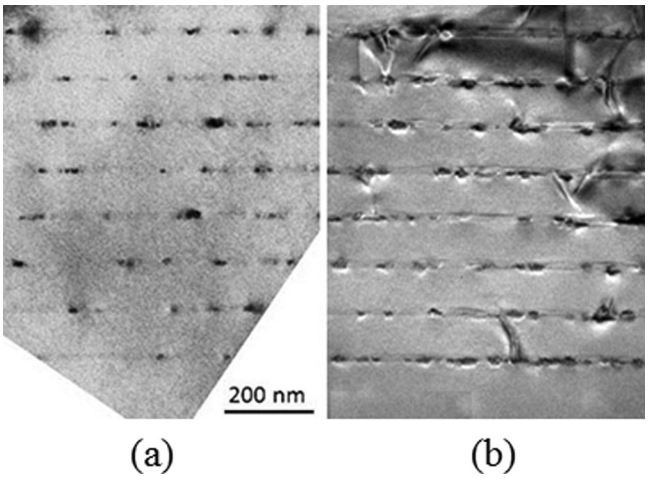

FIG. 5. High-resolution TEM images of 10 stacked InAs/$Al_{0.3}Ga_{0.7}As$ QD layers using capping methods A and B. Plastic deformation resulting in threading dislocations is evident in B.

dislocation loops (Fig. 6(b)). Some of the 60° dislocations do not close into a loop around the InAs QD and are observed in Fig. 5(b) to thread along {111} planes into the barrier layer. Thus, when coverage method A is applied (in Fig. 5(a)), the density of small dots with lateral dimensions of ~10 nm is higher and the layer structure does not show threading dislocations. In contrast, for method B (in Fig. 5(b)), threading 60° dislocations are observed originating from some of the larger quantum dots.

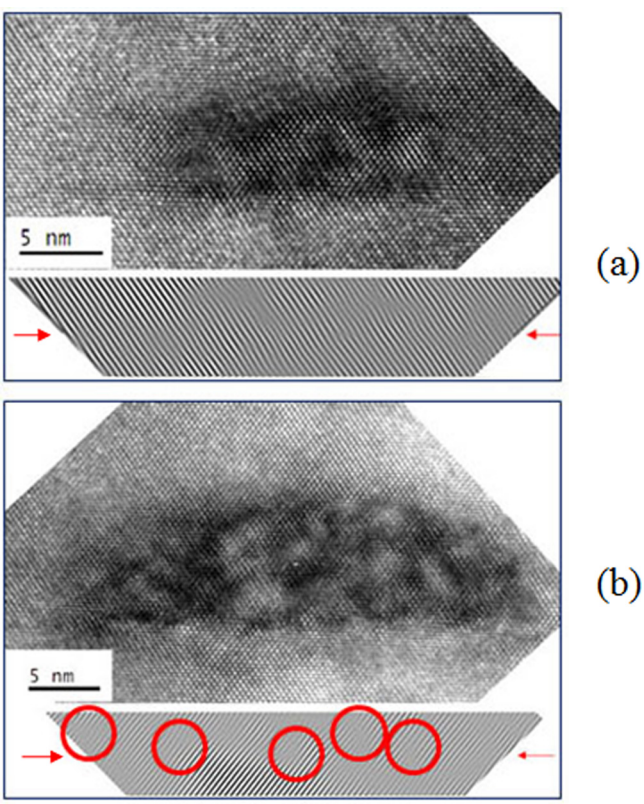

FIG. 6. High-resolution TEM images of InAs QDs on $Al_{0.3}Ga_{0.7}As$ for (a) small and (b) large QDs. Fourier-filtered images of the interface region, using a set of {111} planes, show the presence of extra planes (i.e., misfit dislocations) in (b) but not in (a).

Misfit dislocations have been observed for both coverage methods, especially associated with larger QDs. However, for method A, the dislocations are confined forming a closed loop around the QDs, while for method B some of the dislocations propagate from one layer to another as threading dislocations. During the In-flush step of method A, the exposed indium removal is assisted by the higher temperature, and islands taller than 5 nm are typically truncated and converted into disks.[10] Method B is different in that the temperature is raised only after 20 nm of GaAs is grown at a lower temperature, resulting in complete capping of the dots. Strain due to different island heights may result in the observed bimodal size distribution in Fig. 4(c). Large islands improperly capped would have some misfit dislocations that do not close into loops and instead propagate with the growth surface in Fig. 5(b).

We have used RAS spectra to evaluate both coverage methods for the 5 stacked layers of InAs QDs embedded in $Al_{0.3}Ga_{0.7}As$ (Fig. 7). As the QDs are grown, the surface is observed to evolve from a (4×4) (001) surface reconstruction to a (2×4)-like InAs surface. The (2×4) reconstruction is expected for two-dimensional InAs; but in this case, the relative maximum peak in the RAS spectrum is shifted from 2.3 to 2.5 eV due to tensile strain.[26] Figure 7(a) shows the RAS spectrum of InAs QDs on AlGaAs taken at 400 °C for the first and for the last QD layers. The spectra are almost equal indicating that the reconstruction is not affected by the bottom QD layers when capping method A is used. For method B in Fig. 7(b), a slight difference can be observed between the spectra of the first and the last QD layers. An

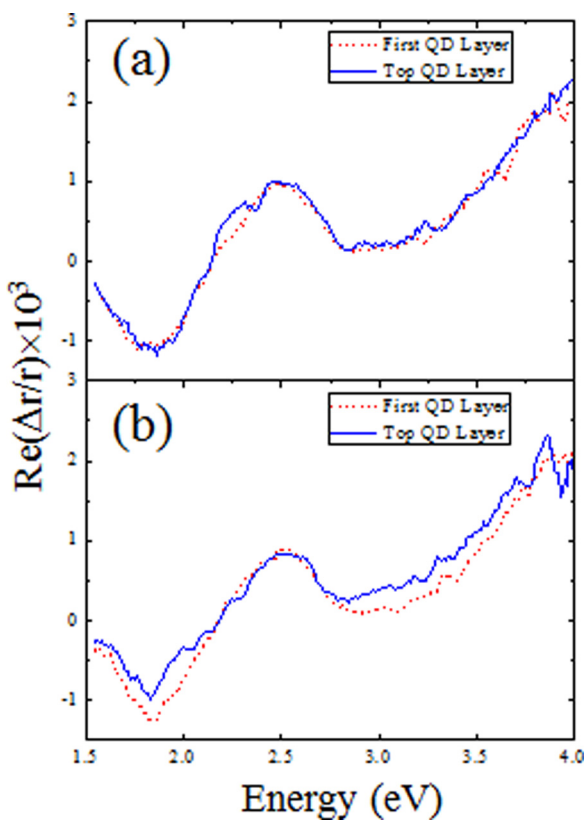

FIG. 7. RAS spectra of the first and last QD layers in a 5 stacked layers of InAs/$Al_{0.3}Ga_{0.7}As$ QDs using (a) capping method A, and (b) capping method B.

[This article is copyrighted as indicated in the article. Reuse of AIP content is subject to the terms at: http://scitation.aip.org/termsconditions. Downloaded to] IP: 149.169.162.2 On: Tue, 17 Feb 2015 22:23:12

increase of the RAS signal is evident for the QD top layer at energies higher than 2.7 eV, which is attributed to the enhancement of anisotropy and the presence of larger islands.[26]

PL measurements performed at low temperatures (10 K) on these InAs QDs layer structures are shown in Fig. 8. The sample with coverage method A shows emission peaks at 1.261 and 1.309 eV in Fig. 8(a). These can be associated to transitions from the VB to the IB. The appearance of two energies may result from a bimodal size distribution or to QD excited states. On the other hand, these emissions are not evident or appear to spread out from 1.36 to below 1.0 eV in the samples without In-flush (from 915 to >1200 nm in Fig. 8(b)), consistent with a large size inhomogeneity. The higher energy emissions at 1.38 and 1.42 eV (900 and 870 nm) that appear in the samples prepared using methods A and B, respectively, are attributed to indium surface diffusion from the InAs QDs into the thin GaAs layers used to cover the dots.[27] In fact, the energy gap of GaAs at 10 K is around 1.5 eV and the observed lower energies are consistent with InGaAs formation due to In incorporation in GaAs layer. The PL emission at ~1.30 and 1.26 eV is interpreted as being transitions between the VB and the IB. These energies are close to the calculated value for dots of 6 nm height at 0 K. It is important to note that our calculation model is only an approximated description and can be refined by introducing strain effects. Moreover, as already mentioned, we should more correctly relate to energy range transitions due to the IB formation. However, for quantum dots 5 nm high, we would expect a transition energy E_M at room temperature of about 1.35 eV close to the theoretically ideal 1.24 eV value for IBSC applications.

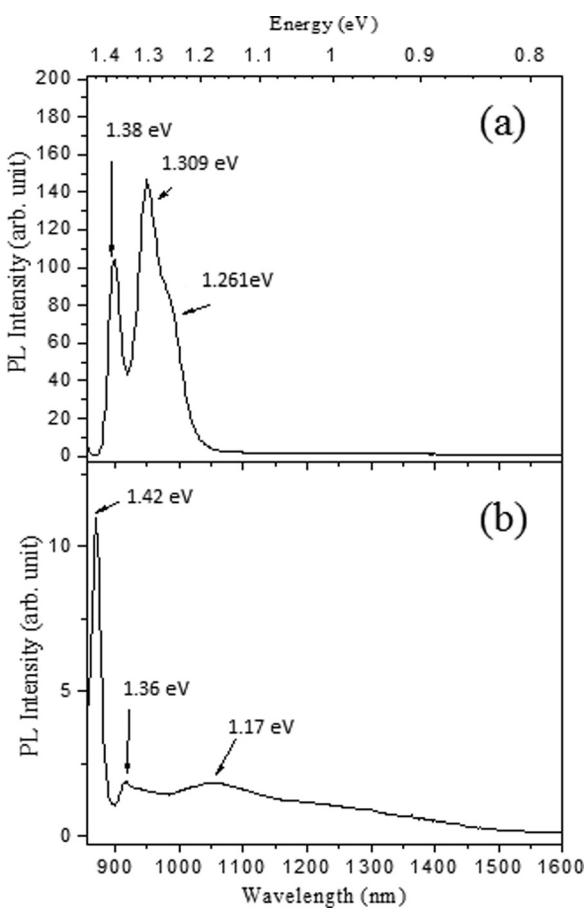

FIG. 8. Photoluminescence spectra at 10 K of 5 stacked layers of InAs/$Al_{0.3}Ga_{0.7}As$ QDs using (a) capping method A, and (b) capping method B. Relative intensities are maintained in the figures.

IV. CONCLUSIONS

In this paper, we have investigated multilayers of InAs QDs separated by $Al_{0.3}Ga_{0.7}As$ thin films. Theoretical calculations show that the use of this barrier material is suitable to approach the ideal transition energy combination for IBSC. We have established appropriate MOVPE growth conditions for InAs/AlGaAs in order to improve the QD size-homogeneity and density. We have also compared two different QD capping methods and have concluded that the In-flush approach is crucial to preserve size uniformity and prevent QD coalescence and height increase from layer to layer, even in the case of a relatively thick, 90-nm, spacer layer for which the dots are not vertically correlated. The influence of the capping method on the structure is further put into evidence by TEM images, from which it becomes clear that the In-flush is effective in suppressing threading dislocations in the stacked InAs/$Al_{0.3}Ga_{0.7}As$ QD layer structure. We have also observed the influence of the capping method on the QD reconstruction by RAS. Independently from the capping method, the surface reconstruction during QDs growth is typical of strained InAs. However, if QDs are not subjected to In-flush, the RAS spectra suggest the formation of larger islands. In addition, samples subjected to In-flush also exhibit the desirable optical properties, with strong PL emission around 1.26–1.3 eV at 10 K which is associated to the transition between VB and the IB (E_M), and correspond to about 1.35 eV at room temperature (the operating conditions of solar cells), close to the ideal 1.24 eV value. The growth of stacked InAs/$Al_{0.3}Ga_{0.7}As$ QD layer structures with appropriate uniformity, high density, adequate structural property, and the correct optical transition energy is an important step towards the fabrication of QD-IBSCs with improved efficiency.

ACKNOWLEDGMENTS

This work was partially supported by Fundação de Amparo a Pesquisa do Estado de Rio de Janeiro (*FAPERJ*) and Conselho Nacional de Desenvolvimento Científico e Tecnológico (CNPq). The research at ASU was supported in part by the National Science Foundation (NSF) and the Department of Energy (DOE) under NSF CA No. EEC-1041895, and in part by the NSF Materials World Network (DMR-1108450).

[1]F. Heinrichsdorff, M. H. Mao, N. Kirstaedter, A. Krost, D. Bimberg, A. O. Kosogov, and P. Werner, Appl. Phys. Lett. **71**, 22 (1997).
[2]O. B. Shchekin and D. G. Deppe, Appl. Phys. Lett. **80**, 3277 (2002).
[3]Z. Chen, O. Baklenov, E. T. Kim, I. Mukhametzhanov, J. Tie, Z. Ye, and J. C. Campbell, J. Appl. Phys. **89**, 4558 (2001).

[This article is copyrighted as indicated in the article. Reuse of AIP content is subject to the terms at: http://scitation.aip.org/termsconditions. Downloaded to] IP: 149.169.162.2 On: Tue, 17 Feb 2015 22:23:12

[4]K. Sears, J. Wong-Leung, M. Buda, H. H. Tan, and C. Jagadish, in *2006 International Conference on Nanoscience and Nanotechnology* (2006), Vol. 1–2, p. 578.
[5]K. Pötschke, L. Müller-Kirsch, R. Heitz, R. L. Sellin, U. W. Pohl, D. Bimberg, N. Zakharov, and P. Werner, Physica E **21**, 606 (2004).
[6]R. Kremzow, M. Pristovsek, and M. Kneissl, J. Cryst. Growth **310**, 4751 (2008).
[7]G. Saint-Girons, G. Patriarche, A. Mereuta, and I. Sagnes, J. Appl. Phys. **91**, 3859 (2002).
[8]A. A. Khandekar, G. Suryanarayanan, S. E. Babcock, and T. F. Kuech, J. Cryst. Growth **292**, 40 (2006).
[9]T. Yang, J. Tatebayashi, M. Nischicka, and Y. Arakawa, Physica E **40**, 2182 (2008).
[10]Z. R. Wasilewski, S. Fafard, and J. P. McCaffrey, J. Cryst. Growth **201/202**, 1131 (1999).
[11]A. Luque and A. Martí, Phys. Rev. Lett. **78**, 5014 (1997).
[12]A. Luque, A. Martí, and C. Stanley, Nature Photonics **6**, 146 (2012).
[13]I. Ramiro, E. Antolin, M. J. Steer, P. G. Linares, E. Hernandez, I. Artacho, E. Lopez, T. Ben, J. M. Ripalda, S. I. Molina, F. Briones, C. R. Stanley, A. Martí, and A. Luque, in 38th IEEE Photovoltaic Specialists Conference (PVSC) (2012), p. 000652.
[14]A. Luque, P. G. Linares, E. Antolin, I. Ramiro, C. D. Farmer, E. Hernandez, I. Tobias, C. R. Stanley, and A. Martí, J. Appl. Phys. **111**, 044502 (2012).
[15]D. Guimard, R. Morihara, D. Bordel, K. Tanabe, Y. Wakayama, M. Nishioka, and Y. Arakawa, Appl. Phys. Lett. **96**, 203507 (2010).
[16]B. C. Richards, L. Yong, P. Pate, D. Chumney, P. R. Sharps, C. Kerestes, D. Forbes, K. Driscoll, A. Podell, and S. Hubbard, in 38th IEEE Photovoltaic Specialists Conference (PVSC), 2012.
[17]A. Mellor, A. Luque, I. Tobías, and A. Martí, Appl. Phys. Lett. **101**, 133909 (2012).
[18]E. Antolín, A. Marti, C. D. Farmer, P. G. Linares, E. Hernandez, A. M. Sanchez, T. Ben, S. I. Molina, C. R. Stanley, and A. Luque, J. Appl. Phys. **108**, 064513 (2010).
[19]S.-S. Li, J. B. Xia, Z. L. Yuan, and Z. Y. Xu, Phys. Rev. B **54**, 11575 (1996).
[20]I. Vurgaftman, J. R. Meyer, and L. R. Ram-Mohan, J. Appl. Phys. **89**, 5815 (2001).
[21]O. Madelung, *Semiconductors: Data Handbook* (Springer, Berlin, 2004), pp. **94**, 118, 148.
[22]M. H. Degani and M. Z. Maialle, J. Comput. Theor. Nanosci. **7**, 454 (2010).
[23]B. Bansal, M. R. Gokhale, A. Bhattacharya, and B. M. Arora, J. Appl. Phys. **101**, 094303 (2007).
[24]A. A. El-Emawy, S. Birudavolu, P. S. Wong, Y. B. Jiang, H. Xu, S. Huang, and D. L. Huffaker, J. Appl. Phys. **93**, 3529 (2003).
[25]L. Hoeglund, E. Petrini, C. Asplund, H. Malm, J. Y. Andersson, and P. O. Holtz, Appl. Surface Science **252**, 5525 (2006).
[26]E. Steimetz, J. T. Zettler, F. Schienle, T. Trepk, T. Wethkamp, W. Richter, and I. Sieber, Appl. Surf. Sci. **107**, 203 (1996).
[27]V. D. Dasika, J. D. Song, W. J. Choi, N. K. Cho, J. I. Lee, and R. S. Goldman, Appl. Phys. Lett. **95**, 163114 (2009).

[This article is copyrighted as indicated in the article. Reuse of AIP content is subject to the terms at: http://scitation.aip.org/termsconditions. Downloaded to] IP: 149.169.162.2 On: Tue, 17 Feb 2015 22:23:12